A Comparative Study of Peptide Models of the α-Domain of α-Lactalbumin, Lysozyme, and α-Lactalbumin/Lysozyme Chimeras Allows the Elucidation of Critical Factors That Contribute to...

6 AUTHORS, INCLUDING:

Shuiqin Zhou
City University of New York - College of State…

105 PUBLICATIONS 4,264 CITATIONS

SEE PROFILE

Robert Fairman
Haverford College

78 PUBLICATIONS 3,733 CITATIONS

SEE PROFILE

Benjamin Chu
Stony Brook University

677 PUBLICATIONS 21,036 CITATIONS

SEE PROFILE

A Comparative Study of Peptide Models of the α-Domain of α-Lactalbumin, Lysozyme, and α-Lactalbumin/Lysozyme Chimeras Allows the Elucidation of Critical Factors That Contribute to the Ability to Form Stable Partially Folded States[†]

Stephen J. Demarest,[‡] Shui-Qin Zhou,[‡] James Robblee,[§] Robert Fairman,[§] Benjamin Chu,[‡] and Daniel P. Raleigh*,[‡]

*Department of Chemistry, State University of New York at Stony Brook, Stony Brook, New York 11794-3400,
Department of Molecular, Cell and Developmental Biology, Haverford College, Haverford, Pennsylvania 19041, and
Graduate Program in Biophysics and Graduate Program in Molecular and Cellular Biology, State University of Stony Brook,
Stony Brook, New York 11794*

ABSTRACT: α-Lactalbumin (αLA) forms a well-populated equilibrium molten globule state, while the homologous protein hen lysozyme does not. αLA is a two-domain protein and the α-domain is more structured in the molten globule state than is the β-domain. Peptide models derived from the α-subdomain that contain the A, B, D, and 3_{10} helices of αLA are capable of forming a molten globule state in the absence of the remainder of the protein. Here we report comparative studies of a peptide model derived from the same region of hen lysozyme and a set of chimeric α-lactalbumin−lysozyme constructs. Circular dichroism, dynamic light scattering, sedimentation equilibrium, and fluorescence experiments indicate that the lysozyme construct does not fold. Chimeric constructs were prepared to probe the origins of the difference in the ability of the two isolated subdomains to fold. The first consists of the A and B helices of αLA cross-linked to the D and C-terminal 3_{10} helices of lysozyme. This construct is highly helical, while a second construct that contains the A and B helices of lysozyme cross-linked to the D and 3_{10} helices of αLA does not fold. Furthermore, the disulfide cross-linked homodimer of the αLA AB peptide is helical, while the homodimer of the lysozyme AB peptide is unstructured. Thus, the AB helix region of αLA appears to have an intrinsic ability to form structure as long as some relatively nonspecific interactions can be made with other regions of the protein. Our studies show that the A and B helices plays a key role in the ability of the respective α-subdomains to fold.

A growing number of proteins have been shown to form partially folded states that are stable under mildly denaturing conditions (*1−5*). These states, commonly referred to as molten globules, are thought to resemble partially folded structures populated during the folding process (*3, 6−8*). Molten globule states are compact with modest to large amounts of presumably nativelike secondary structure, but have a dynamic nature and lack the fixed tertiary interactions characteristic of fully folded proteins. Some proteins have been shown to populate an additional compact stable equilibrium state with properties intermediate between those of the classic molten globule and the unfolded state (*9−11*). The term pre-molten globule state has been coined to describe these structures (*9*). Elucidation of the structure of partially folded states such as the molten globule and the determination of the interactions that stabilize these partially folded structures is an active area of research.

This paper is primarily concerned with the origin of the difference in the equilibrium unfolding behaviors of human α-lactalbumin (αLA)[1] and hen lysozyme. The C-type lysozymes and α-lactalbumins are evolutionarily linked and have very similar folded structures (Figure 1) (*12−14*). Their structure consists of two domains, a helical domain known as the α-domain, composed of four α-helices (A through D) and a 3_{10} helix, and a sheet/coil domain known as the β-domain. Both proteins form intermediates during folding (*15, 16*), but they exhibit very different equilibrium unfolding behaviors. All α-lactalbumins investigated thus far including the human protein form a molten globule state that is stable under a variety of conditions. In contrast, the most extensively studied of the c-type lysozymes, hen lysozyme (*14*),

[1] Abbreviations: αLA, α-lactalbumin; ANS, 1-anilinonaphthalene-8-sulfonate; CD, circular dichroism; GuHCl, guanidinium hydrochloride; HPLC, high-pressure liquid chromatography; PAL, 5-(4′-Fmoc-aminomethyl-3′,5′-dimethoxyphenoxy) valeric acid; PSV, partial specific volume; R_g, radius of gyration; R_h, hydrodynamic radius; TBTU, O-(7-benzotriazol-1-yl)-1,1,3,3-tetramethyluronium tetrafluoroborate; TFA, trifluoroacetic acid.
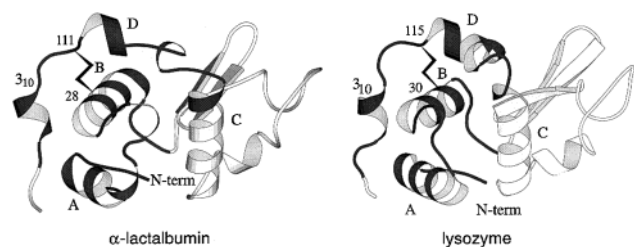
FIGURE 1: Ribbon diagrams of human αLA and hen lysozyme created using MOLSCRIPT (60). The helices in the α-domain are labeled. The disulfide bond that links the B and D helices is labeled. The regions included in the peptide constructs are shaded gray.

normally displays two-state equilibrium unfolding transitions when denatured by pH, chemical denaturants, or temperature (*17*, *18*).

Studies of αLA have shown that the α-domain is structured in the molten globule state, while the β-domain is less ordered (*19–25*). Kim and co-workers have demonstrated that the isolated α-domain (residues 1–39 and 81–123 connected by a glycine linker) is able to fold to a molten globule-like structure even in the absence of the β-domain (*23*). We have shown that the region corresponding to the C helix is not required for the α-domain to form a molten globule state (*24*). Our studies have demonstrated that a peptide composed of residues 1–38, which encompasses the A and B helices, cross-linked by the native 28–111 disulfide bond to a peptide corresponding to residues 95–120, which includes the D and 3_{10} helices, is sufficient to fold to a highly helical molten globule state. This construct has been denoted αLA:1–38/95–120. Deletion of residues 95–100 from this construct has no effect upon its structure although it does slightly reduce its resistance to urea denaturation. Further truncation, however, results in a drastic loss of structure. Deletion of the region of the polypeptide chain that corresponds to the A helix, or the D helix or the C-terminal 3_{10} helix leads to constructs that are largely unfolded (*24*). These studies have demonstrated that the region of the α-domain that includes the A, B, D, and 3_{10} helices comprises a critical core whose integrity appears to be required for the formation of the αLA molten globule state.

In this work, we use circular dichroism (CD), fluorescence, light scattering, ANS binding measurements, and sedimentation equilibrium experiments to characterize a 70-residue peptide model that encompasses the same region of hen lysozyme. The peptide includes one fragment encompassing the region of the A and B helices (denoted lys:1–40) cross-linked via the native 30 to 115 disulfide bond to another peptide corresponding to residues 98–127 that includes the D and C-terminal 3_{10} helices (designated lys:98–127) (Figure 1). The primary sequences of both the αLA and lysozyme peptides are shown in Figure 2. The oxidized lysozyme peptide construct is denoted lys:1–40/98–127. We also study a set of chimeric peptides that are composed of fragments of αLA cross-linked to fragments of lysozyme. Comparison of the properties of these constructs to our previously characterized all αLA construct and to the lysozyme construct provides new insight into the factors that lead to a stable molten globule state.

Studies with chimeras allow entire units of secondary structure to be transplanted and can provide insight into the relative importance of the various units of secondary structure
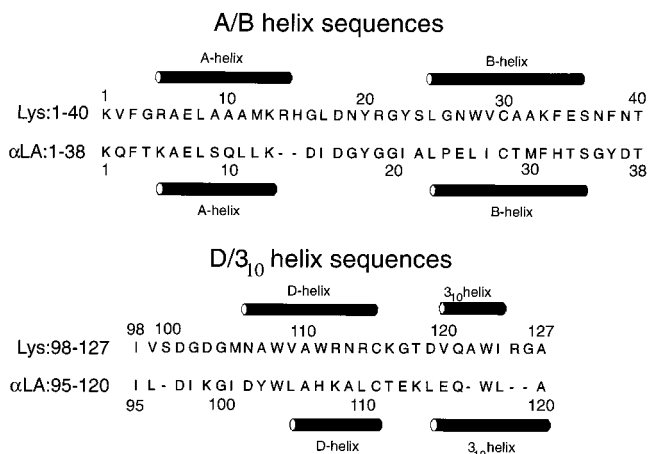

FIGURE 2: Primary sequences of lys:1–40, αLA:1–38, lys:98–127, and αLA:95–120. The location of the native helices in the primary sequence are indicated by cylinders above or below the sequences. The standard alignment of Acharya and co-workers was used (*61*).

and of the interactions between these units. A chimeric construct of hen lysozyme and bovine αLA has previously been used to probe the differential Ca^{2+} binding properties of the two proteins (*26*). In another study, a six-residue sequence derived from the D helix region of equine lysozyme was transplanted into human αLA to test how disrupting potential non-native interactions in human αLA might alter the stability of the molten globule state (*27*). Chimeric constructs in which entire subdomains of human and bovine of α-LA have been combined have been used to study the difference in the stability of the molten globule states of human and bovine α-LA (*28*, *29*). In this work, we analyze two hybrid peptide constructs. One denoted lys:1–40/αLA: 95–120 consists of a peptide containing the first 40 residues of lysozyme cross-linked to a peptide containing residues 95–120 of αLA. This peptide contains the A and B helices of lysozyme and the D and 3_{10} helices of αLA. The second chimera is denoted αLA:1–38/lys:98–127. It is composed of the peptide corresponding to the first 38 residues of αLA cross-linked to residues 98–127 of lysozyme. This molecule includes the A and B helices from αLA and the D and 3_{10} helices from lysozyme. We also characterize the oxidized homodimers derived from the various αLA and lysozyme peptides. These molecules were isolated during the preparation of the cross-linked heterodimers and certain interesting trends were observed in their propensity to form structure.

In addition, we report the results of dynamic light scattering experiments that allow us to probe the compactness of the αLA and lysozyme constructs. Our previous studies of the αLA construct made use of CD and fluorescence and provided excellent evidence that it formed a molten globule, but they did not provide any direct information about the compactness of the molecule (*24*). The light scattering experiments described in this work provide a direct measure of the compactness and both complement and extend our previous studies.

MATERIALS AND METHODS

Synthesis and Purification. Lys:1–40 and lys:98–127 were designed with the native Cys residues at positions 6 and 127 replaced by Ala. Peptide synthesis reagents were

purchased from PerSeptive Biosystems Inc. or Advanced ChemTech. Solvents were purchased from Fisher Scientific. Lys:1−40 and lys:98−127 were synthesized on a 0.2-mmol scale using a Millipore 9050 automated peptide synthesizer. Fmoc-L-amino acids were coupled via O-(7-benzotriazol-1-yl)-1,1,3,3-tetramethyluronium tetrafluoroborate (TBTU) activation. The use of a peptide amide linker (PAL resin) provided amidated carboxy-termini. The amino-termini of lys:98−127 and αLA:95−120 were acetylated, while lys:1−40 and αLA:1−38 have free amino-termini. Peptides were cleaved from the resin using a solution of 90% TFA, 3.3% ethanedithiol, 3.3% anisole, and 3.3% thioanisole. The peptides were purified using reverse phase HPLC with H$_2$O/CH$_3$CN gradients containing 0.065% HCl with a Vydac C18 column. The identities of the peptide fragments were confirmed using MALDI TOF mass spectrometry. The synthesis and purification of αLA:1−38 and αLA:95−120 have been described elsewhere (*24*). The peptide fragments were cross-linked via air oxidation for 24 h in aqueous solution at pH 8.5 and purified by reverse phase HPLC. All of the oxidation reactions led to a simple pattern of three peaks on the HPLC trace that represented two homodimers and one heterodimer. Peak identification was achieved using MALDI TOF mass spectrometry. The peptide constructs and reduced peptide fragments were all greater than 95% pure as judged by analytical HPLC.

Circular Dichroism. CD measurements were conducted using an Aviv model 62A circular dichroism spectrometer. Wavelength scans were performed with a minimum of three repeats and an averaging time of 3 s. A 2 mM phosphate, 2 mM borate, 2 mM citrate buffer containing 10 mM NaCl was used for all CD experiments. Concentration dependence studies were performed by dilution from a concentrated peptide stock solution into this buffer. All CD and fluorescence experiments were performed at pH 2.8, 25 °C unless otherwise stated in the text. The concentration of the stock solutions were determined by absorbance measurements at 280 nm using extinction coefficients calculated by the method of Pace and co-workers (*30*).

Sedimentation Equilibrium. The oxidized constructs (lys:1−40/98−127, lys:1−40/αLA:95−120, and αLA:1−38/lys:98−127) were dialyzed against 2 mM phosphate, 2 mM borate, 2 mM citrate, 10 mM NaCl solution at pH 2.8. Sedimentation equilibrium experiments were performed at 25 °C using a Beckman XL-A analytical ultracentrifuge at rotor speeds of 30 000, 40 000, and 50 000 rpm. Experiments were performed at two concentrations, 10 and 4 μM. These experiments were carried out using 12-mm path length, six-channel, charcoal-filled, Epon cells with quartz windows. Partial specific volumes were calculated from the weighted average of the partial specific volumes of the individual amino acids (*31*). The data were globally fit with a single species model with the molecular weight treated as a fitting parameter. The HID program from the Analytical Ultracentrifugation Facility at the University of Connecticut was used for the fitting analysis.

Dynamic Laser Light Scattering Measurements. A standard laboratory-built laser light scattering spectrometer equipped with a BI-9000 AT digital correlator (Brookhaven Instrument Inc.) and a solid-state laser (DPSS, Coherent, 200 mW, 532 nm) was used to perform the dynamic light scattering. The scattering cell was held in a brass thermostat block filled

with a refractive index matching silicone oil. The temperature was controlled to within ± 0.05 °C. The intensity−intensity time correlation function $G^{(2)}(t,q)$ in the self-beating mode was measured at a scattering angular range of 30−60°. To perform light scattering measurements for low molecular weight proteins at very dilute concentrations in aqueous media is very difficult experimentally. We used a 0.1 μM Millex-VV filter to remove dust from the sample. A time period of 24−28 h was used to get smooth scattering curves. $G^{(2)}(t,q)$ can be related to the electric field time correlation function $g^{(1)}(t,q)$ as

$$G^{(2)}(t,q) = A[1 + \beta |g^{(1)}(t,q)|^2]$$

where A is the baseline; β, a parameter depending on the coherence of the detection; t, the delay time; and q is equal to $4\pi n/\lambda \sin(\theta/2)$ with n, λ, and θ being the refractive index of the solvent, wavelength of the incident beam in a vacuum, and scattering angles, respectively. $g^{(1)}(t,q)$ is further related to the characteristic line width (Γ) by

$$g^{(1)}(t,q) = \int_0^\infty G(\Gamma)e^{-\Gamma t}d\Gamma$$

By using both a cumulants method and a CONTIN program, $G(\Gamma)$ could be calculated. Furthermore, we could obtain the translational diffusion coefficient D from Γ by using the relationship, $D = \Gamma/q^2$. Once D is determined, the hydrodynamic radius, R_h, can be obtained by the Stokes−Einstein equation

$$R_h = k_B T/6\pi\eta D$$

with T, k_B, and η being the absolute temperature, the Boltzmann constant and the solvent viscosity, respectively. The experiments were conducted using the same buffer system that was used in the CD experiments. The concentration of GuHCl in the unfolded sample of αLA:1−38/95−120 was determined by the measured refractive index of the solution, 1.374. The solvent viscosity of the 2.4 M GuHCl sample was also directly measured and found to be 0.954 centipoise.

Fluorescence Measurements. All fluorescence measurements were performed using an ISA Fluorolog spectrometer. Trp fluorescence experiments were performed using an excitation wavelength of 280 nm. Emission spectra were recorded over the range of 285 to 450 nm. ANS fluorescence experiments were performed using an excitation wavelength of 370 nm. Emission spectra were recorded over the range of 380 to 650 nm. The concentration of the ANS stock solution was determined using a molar absorption coefficient of 8.0×10^3 M^{-1} cm^{-1} at 372 nm in methanol (provided by Molecular Probes). The stock solution was diluted into buffer at pH 2.8 yielding a final ANS concentration of 2 μM. The peptides were titrated into this solution.

Analysis of the Primary Sequences. The total nonpolar and polar accessible surface areas of the peptide constructs were calculated using the access module in the program WHAT IF (http://swift.EMBL-Heidelberg.DE/whatif/) using a 1.4-Å probe radius. The unfolded state of each of the peptide constructs were modeled as extended chains with ϕ and ψ equal to 180°. All carbon and sulfur atoms were considered nonpolar. Nitrogen and oxygen were considered to be polar.
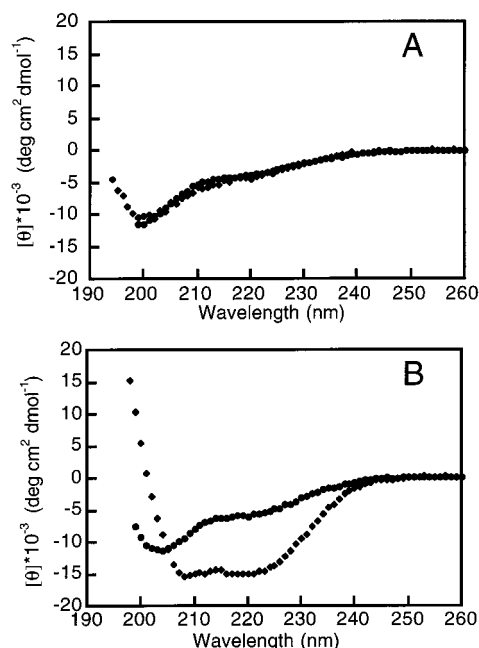
FIGURE 3: CD spectra of (A) the oxidized (diamonds) and reduced (circles) forms of lys:1−40/98−127 and (B) the oxidized (diamonds) and reduced (circles) forms of αLA:1−38/95−120. All experiments were performed at 25 °C, pH 2.8. The CD spectra of the reduced forms of the peptide constructs were derived from the sum of the spectra of the isolated peptides and normalized for the number of peptide bonds.

Packing densities were determined using the algorithm of Fleming and co-workers (*32, 33*). The local helix propensity was calculated using the AGADIR algorithm of Serrano (*34, 35*).

RESULTS

The Lysozyme Construct, lys:1−40/98−127, Is Unfolded. Both lys:1−40 and lys:98−127 have a very small tendency to form structure in isolation as judged by CD. The N-terminal fragment, lys:1−40, and the C-terminal fragment, lys:98−127, both display concentration-dependent changes in their CD spectra above 10 μM peptide. At 4 μM, lys:1−40 and lys:98−127 have $[\theta]_{222}$ values of −3300 and −4000 deg cm^2 dmol^{-1}, respectively, at pH 2.8, 25 °C (data not shown). Only a small amount of helical structure would be required to account for the observed CD values. Somewhat similar results have been reported by Yang et al. who studied a slightly different set of lysozyme peptides at higher concentrations (*36, 37*). These workers also studied the 1−40 fragment of hen lysozyme, and they also observed that it was largely unstructured.

Analytical ultracentrifugation measurements indicate that the oxidized heterodimer, lys:1−40/98−127, is monomeric at concentrations of 4 μM and below. Small amounts of higher order aggregates begin to form at 10 μM. Therefore, all experiments were performed using peptide concentrations of 4 μM and below. Cross-linking the two lysozyme peptides by the native 30 to 115 disulfide does not induce any additional structure (Figure 3). At pH 2.8 and 25 °C, the intensity of the helical band of the CD spectrum at 222 nm is −3800 deg cm^2 dmol^{-1} after oxidation, while the normalized sum of the values of $[\theta]_{222}$ of the two reduced peptides is −3600 deg cm^2 dmol^{-1}. The fluorescence emission

spectrum provides additional evidence for the lack of structure. The emission maximum of each of the reduced peptides is 355 ± 1 nm and it is 354 ± 1 nm for lys:1−40/98−127. This is very close to the emission maximum observed for intact lysozyme at pH 2.8, 25 °C in 10 M urea, 356 nm. These results indicate that the Trp residues are not sequestered from solvent and are consistent with the CD studies. The behavior of the lysozyme peptide construct is dramatically different than the behavior of the αLA peptide construct. Cross-linking the related αLA peptides resulted in a significant increase in helical structure and a notable blue shift in the fluorescence emission maximum (*24*).

We have analyzed lys:1−40/98−127 in the presence of Na$_2$SO$_4$, a reagent known to stabilize proteins. The construct was also studied at low temperature, as well as at pH 7.0. These experiments were conducted to determine whether a structured conformation is only marginally unstable and might be induced by changing the solvent conditions. There is no significant increase in the value of $[\theta]_{222}$ in the presence of Na$_2$SO$_4$ up to a concentration of 1 M; although visible aggregates were observed at Na$_2$SO$_4$ concentrations above 0.3 M. Raising the pH to 7.0 does not induce additional structure in lys:1−40/98−127. The value of $[\theta]_{222}$ of the oxidized construct is −4800 deg cm^2 dmol^{-1} at pH 7.0. The normalized sum of $[\theta]_{222}$ of the two reduced peptides is −4200 deg cm^2 dmol^{-1}. Lowering the temperature also failed to induce any significant structure; the value of $[\theta]_{222}$ of lys:1−40/98−127 is only −4200 deg cm^2 dmol^{-1} at pH 2.8, 1 °C.

A common feature of molten globule states is their ability to bind the fluorescent hydrophobic dye ANS (*38*). The highly helical αLA construct, αLA:1−38/95−120, binds ANS (*24*). The reduced lys:98−127 peptide did not bind ANS (5 μM peptide, 2 μM ANS), while the reduced lys:1−40 peptide bound ANS weakly. The fluorescence intensity of the ANS increased 2.5-fold upon the addition of 5 μM lys:1−40 and the emission maximum shifted to 477 nm. Yang et al. observed strong ANS binding to a peptide consisting of residues 84−129 of hen lysozyme in an experiment performed at higher peptide and ANS concentrations (*36*). Both lys:1−40 and lys:98−127 displayed concentration-dependent changes in their CD spectra above 10 μM peptide concentrations, and therefore we carried out our ANS binding experiments at lower peptide and ANS concentrations. Lys:1−40/98−127 binds ANS even though the oxidized construct is largely unfolded. Addition of 4 μM lys:1−40/98−127 to a 2-μM ANS solution induces almost a 10-fold increase in ANS fluorescence intensity, and the emission maximum shifts to 471 nm (Figure 4). Although no detectable secondary structure is induced, it appears that formation of lys:1−40/98−127 may lead to the formation of hydrophobic patches or clusters that allow ANS binding. ANS is negatively charged and lys:1−40/98−127 has a net charge of +12 at low pH that might contribute to the binding (*39*); however, ANS binding was still observed when the experiments were repeated in the presence of 750 mM NaCl, indicating that the binding is not simply due to electrostatic interactions.

Characterization of the Hydrodynamic Properties of the Lysozyme and αLA Constructs. The αLA Construct Is Compact, while the Lysozyme Construct is Not. Our previous studies have provided excellent evidence that the αLA
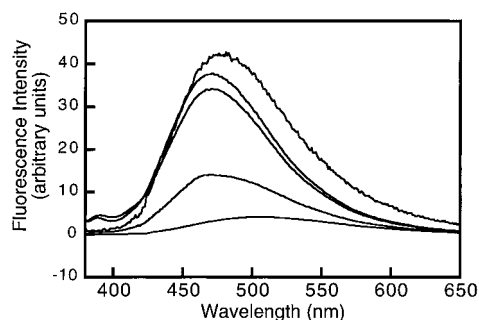
FIGURE 4: Fluorescence emission spectra of 2 μM ANS in the absence of peptide (bottom curve) and in the presence of the four peptide constructs. From top to bottom: 4 μM αLA:1−38/95−120, 4 μM αLA:1−38/lys:98−127, 4 μM lys:1−40/98−127, and 4 μM lys:1−40/αLA:95−120. All experiments were performed at 25 °C, pH 2.8.

construct forms a molten globule-like state, but they did not provide direct information concerning the compactness of the molecule (*24*). Here, we report the results of dynamic light scattering experiments that allow us to determine the hydrodynamic radius, R_h. These are very challenging experiments since they must be performed at very low peptide concentrations to avoid extensive self-association. The R_h of αLA:1−38/95−120 was measured to be 13 ± 2 Å (Figure 5, panel A). Measurement of the radius of gyration (R_g) was not possible using laser light scattering because the particle size is too small to exhibit a measurable angular dependence of the light scattering intensity. The value of R_h for the molten globule state of intact human αLA has been measured by quasielastic light scattering to be 19.9 Å (*40*). αLA:1−38/ 95−120 contains approximately half the number of residues of full-length αLA, and the observed R_h is consistent with the compactness of the molten globule state of the intact protein. The observed value of R_h is noticeably smaller than the value expected for a fully unfolded peptide of the same size. For example, Wilkins et al. have measured an R_h of 15.5 Å for a 37-residue peptide in 8 M urea (*41*). Several empirical correlations that relate the expected value of R_h for the folded and the highly unfolded state to the size of the protein have been reported (*41*, *42*). These relationships were derived by considering single chain proteins, and the constructs examined here consist of two distinct polypeptides cross-linked by a disulfide; nonetheless, it is interesting to compare the experimentally determined values to those predicted by the empirical relationships. The recent correlation published by Dobson and co-workers which relates the size in residues to values of R_h predicts that a single chain 64-residue polypeptide should have a folded state value of R_h on the order of 15.8 Å while a fully unfolded protein of 64 residues is expected to have an R_h on the order of 24 Å (*41*). An earlier relationship due to Uversky relates the expected Stokes radius to the molecular weight and predicts values on the order of 14.8 Å for the Stokes radius of a folded 64-residue protein and a value of 24.6 Å for the highly unfolded state (*42*). We have directly measured the R_h of αLA:1−38/95−120 in 2.4 M GuHCl (Figure 5, panel C). This concentration of GuHCl is sufficient to unfold the construct. In 2.4 M GuHCl, the value of R_h increases to 18 ± 2 Å, which is significantly larger than the value measured in the absence of GuHCl. The R_h of lys:1−40/98−127 in the absence of denaturant was determined to be 17 ± 2 Å
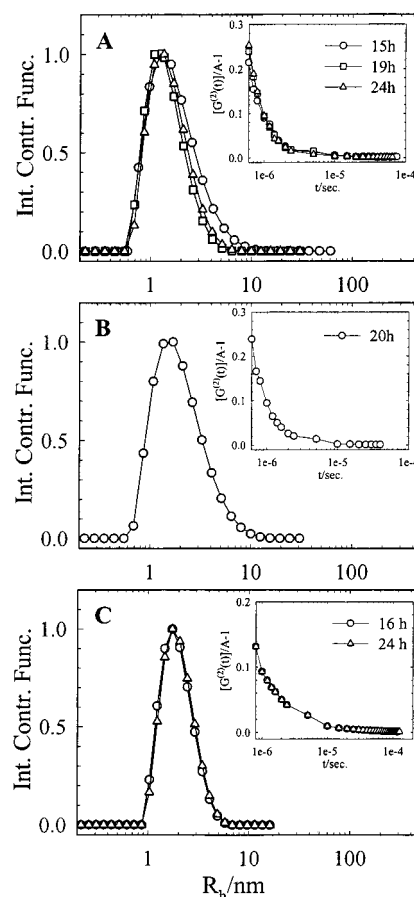

FIGURE 5: Particle size distribution function of (A) αLA:1−38/ 95−120 at pH 2.8, 25 °C after accumulating the light scattering data for 15 h (circles), 19 h (squares), and 24 h (triangles); (B) lys:1−40/98−127 at pH 2.8, 25 °C after accumulating data for 20 h; and (C) αLA:1−38/95−120 at pH 2.8, 25 °C in 2.4 M GuHCl after accumulating data for 16 h (circles) and 24 h (triangles). The inset in each figure displays the intensity−intensity time correlation function curves. The R_h values were calculated to be 13 Å for αLA: 1−38/95−120 in the absence of denaturant, 17 Å for lys:1−40/ 98−127, and 18 Å for αLA:1−38/95−120 in 2.4 M GuHCl with an uncertainty of 2 Å for each measurement.

(Figure 5, panel B). This is considerably larger than the value of R_h measured for the folded form of αLA:1−38/95−120 but is very similar to the value obtained for αLA:1−38/95− 120 in 2.4 M GuHCl. These experiments clearly demonstrate that the αLA construct is compact, while the lysozyme construct is more expanded. The slight asymmetry in the particle size distribution function in the direction of larger particle size seen in Figures 5, panels A and B likely reflects small amounts of association to form higher molecular weight aggregates. This asymmetry will lead to a small overestimate of the average particle size. Thus, the value of 13 ± 2 Å for the R_h of αLA:1−38/95−120 is an upper limit. These results are completely consistent with the CD and fluorescence studies and provide excellent additional evidence that αLA: 1−38/95−120 forms a molten globule like state and lys:1− 40/98−127 does not.

Characterization of the αLA−Lysozyme Chimeric Constructs. Only Constructs That Contain the A and B Helices from αLA are Folded. Our experiments with lys:1−40/98− 127 clearly demonstrate that, as expected, it has a much lower propensity to form structure than does the corresponding αLA construct. We have prepared a set of chimeric peptide
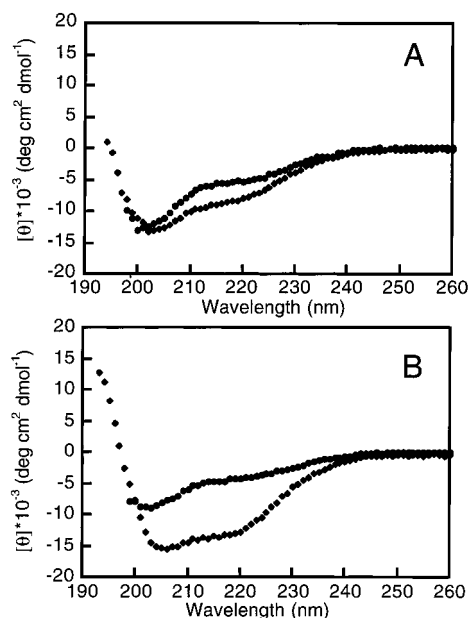
FIGURE 6: CD spectra of (A) the oxidized (diamonds) and reduced (circles) forms of lys:1−40/αLA:95−120 and (B) the oxidized (diamonds) and reduced (circles) forms of αLA:1−38/lys:98−127. All experiments were performed at 25 °C, pH 2.8.

Table 1: Summary of the Experimental Results for the Lysozyme and αLA Peptide Constructs and the Two Chimeric Constructs[a]

peptide construct	$[\theta]_{222}$ (deg cm^2 ·dmol^{-1})	Trp fluor λ_{max} (nm)	ANS fluor λ_{max} (nm)	R_h (Å)
αLA:1−38/95−120	−14 500	345	479	13 ± 2
αLA:1−38/lys:98−127	−11 600	347	471	ND
lys:1−40/αLA:95−120	−7 300	351	470	ND
lys:1−40/98−127	−3 800	354	471	17 ± 2

[a] ANS fluorescence λ_{Max} values are reported for experiments conducted in a solution of 2 μM ANS in the presence of 4 μM peptide. All experiments were conducted at pH 2.8, 25 °C. ND; not determined.

constructs in an effort to understand the origins of the striking differences in the ability of the αLA and lysozyme constructs to fold. The first peptide chimera consists of the A and B helices of αLA (αLA:1−38) cross-linked to the lysozyme D/3$_{10}$ helices (lys:98−127) and is designated αLA:1−38/lys:98−127. The second chimeric peptide construct consists of the lysozyme AB helices (lys:1−40) cross-linked to a peptide that contains the D and 3$_{10}$ helices of αLA (αLA:95−120) and is denoted lys:1−40/αLA:95−120.

Sedimentation equilibrium studies indicate that both of the chimeric peptides are monomeric at pH 2.8, 25 °C at a concentration of 4 μM. Unfortunately, signs of self-association are apparent at concentrations of 10 μM for both peptides and all experiments were conducted at peptide concentrations of 4 μM or below.

Cross-linking the lysozyme AB peptide to the αLA D/3$_{10}$ peptide leads to a marginal increase in structure as judged by CD (Figure 6, panel A, Table 1). The CD spectrum of the construct does exhibit significant intensity at 222 nm; however, much of this signal can be accounted for by the structure present in the isolated αLA:95−120 peptide. Previous studies have shown that the structure in the monomeric form of αLA:95−120 is the result of local, non-native backbone and side chain interactions within the regions encompassed by residues 101−107 and residues 114−120

(43−45). Forming the disulfide cross-link results in only a 1.5-fold increase in the value of $[\theta]_{222}$ relative to the normalized sum of the value of $[\theta]_{222}$ for the two reduced peptides. The Trp fluorescence emission maximum, 351 nm, is weakly blue-shifted from the fluorescence emission maximum of lys:1−40/98−127, 354 nm. The shift is small and is consistent with only a marginal gain in structure allowing for partial or transient burial of the Trp residues. Lys:1−40/αLA:95−120 binds ANS; however, the increase in the ANS fluorescence intensity is approximately a factor of 2.5 less than what is observed for the nonhybrid peptide constructs (Figure 4).

The αLA:1−38/lys:98−127 peptide behaves very differently. A marked increase in structure is observed upon oxidation. The value of $[\theta]_{222}$ increases almost 3-fold from −4100 to −11 600 deg cm^2 dmol^{-1} when the two peptides are cross-linked to one another (Figure 6, panel B, Table 1). This is noticeably larger than the value measured for the other chimera but is smaller than the value measured for αLA:1−38/95−120. Consistent with the far UV CD results, the Trp fluorescence emission maximum of αLA:1−38/lys98−127 is 347 nm. This indicates that αLA:1−38/lys:98−127 forms structure that is capable of partially sequestering the Trp residues from solvent. The emission maximum of this construct is much closer to the value observed for the all αLA construct than for the all lysozyme construct (Table 1). αLA:1−38/lys:98−127 also binds ANS (Figure 4) and the change in ANS fluorescence intensity upon addition of αLA:1−38/lys:98−127 is comparable to that observed for lys:1−40/98−127 and αLA:1−38/95−120 (Figure 4).

Characterization of the Oxidized Homodimers: Only Fragments That Contain the A and B Helices of αLA are Significantly Structured. During the preparation of the various oxidized peptide constructs, we isolated homodimers of αLA:1−38, αLA:95−120, lys:1−40, and lys:98−127. These peptides display interesting trends in their ability to fold. All four homodimers associated at high concentrations, consequently CD experiments were conducted at 4 μM peptide. The αLA:1−38 homodimer is highly helical as indicated by the characteristic double minima at 208 and 222 nm in the CD spectrum (Figure 7). There is almost a 3-fold increase in the value of $[\theta]_{222}$ upon oxidation of αLA:1−38 to form the homodimer. The three other peptides, αLA:95−120, lys:1−40, and lys:98−127 displayed at most, only modest increases in helicity upon formation of a homodimer. The αLA:95−120 homodimer populates a significant amount of structure as judged by CD; however, the reduced αLA:95−120 monomer is already significantly structured, and oxidation to a homodimer leads to only a 30% increase in the value of $[\theta]_{222}$. CD spectra of the homodimers are shown in Figure 7, and a comparison of the values of $[\theta]_{222}$ for each of the reduced peptides and the homodimers is given in Table 2.

The experiments with the chimeric peptides and the homodimers demonstrate that all constructs that contain the αLA AB helix region have a significant propensity to fold. In contrast, all constructs that contain the lysozyme AB helix region are significantly less structured.

Analysis of the Sequences of the Four Peptide Constructs and the Native State of Lysozyme and α-Lactalbumin. The differing ability of the constructs to fold and the differing
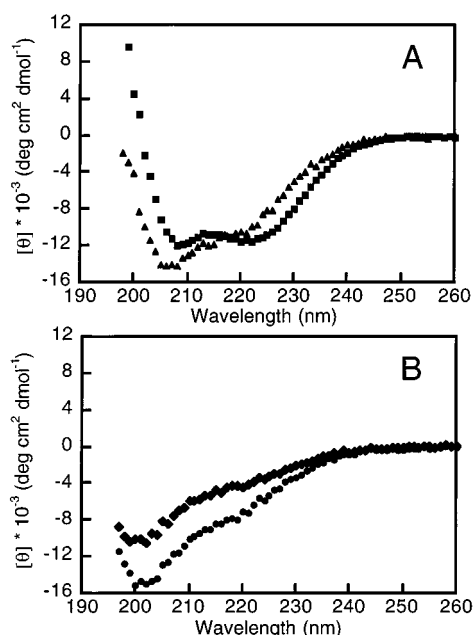
FIGURE 7: (A) CD spectra of the αLA homodimers: The αLA:1−38 homodimer is represented by squares and the αLA:95−120 homodimer by triangles. (B) CD spectra of the lysozyme homodimers: the lys:1−40 homodimer is represented by diamonds and the lys:98−127 homodimer by circles. All experiments were performed at 25 °C, pH 2.8.

Table 2: Comparison of the Intensity of the CD Signal at 222 nm for the Monomeric and Homodimeric Forms of the Lysozyme and αLA Peptides

peptide	$[\theta]_{222}$ monomer (deg cm^2 dmol^{-1})	$[\theta]_{222}$ homodimer (deg cm^2 dmol^{-1})
αLA:1−38	−4000	−11 500
αLA:95−120	−7500	−10 400
lys:1−40	−3000	−3 000
lys:98−127	−4000	−6 300

[a] Measurements were made at pH 2.8, 25 °C.

ability of the full proteins to form stable molten globule states likely depends on the subtle interplay of a variety of factors. In this section, we analyze the primary sequence of the constructs and compare certain features of the native state of lysozyme and αLA in an effort to search for properties that might correlate with the ability to form a molten globule state, paying particular attention to the critical AB helix region. We first consider the potential role of local helical propensity. The region of the polypeptide chain that corresponds to the A helix in human αLA has some propensity to form locally stabilized helical structure as judged by the AGADIR algorithm of Serrano and co-workers (*34, 35*). However, the calculated helical propensity of the same region of lysozyme is also nonzero. The calculated % helix per residue for the segment corresponding to the A helix, residues 5−14 of αLA, ranges from 10 to 24% at pH 2, 278 °C, while the corresponding region of hen lysozyme has values that range from 4 to 18%. Furthermore, the calculated helical propensity for the region corresponding to the B-helix is slightly larger for lysozyme than for αLA, and the overall helix propensity of the N-terminal AB helix region is very similar for the two peptides (5.8 vs 5.1% at pH 2). In addition, the calculated helical propensities of the C-terminal fragments, lys:97−128 and αLA:95−120 are small and are

similar (4.7 vs 2.7%). Experimental studies also suggest that the propensity to form locally stabilized helical structure is not a key determinate of the differing ability of the constructs to fold (*43−46*). Peptide fragments derived from the N-terminal region of αLA and lysozyme are largely unstructured in solution (*36, 46*). The peptide corresponding to the C-terminal portion of the αLA construct does have some tendency to fold in isolation, but the structure is stabilized by non-native interactions, and certain fragments derived from the C-terminal region of the lysozyme sequence also have a tendency to adopt some structure in isolation (*36, 43−45*). Thus, it seems clear that the difference in the ability of the constructs to form structure cannot simply be a result of isolated helix propensities. Recently, somewhat different conclusions concerning the importance of local helical propensities in stabilizing the molten globule state have been reached based on a set of interesting studies of chimeras of bovine and human αLA. A set of chimeras that contained the sequence of the AB helices from the bovine or human protein together with various combinations of the human or bovine D/3$_{10}$ helix region were examined. All of the proteins that contained the AB helices from human αLA were more stable than those that contained the AB helices from the bovine protein (*29*). The calculated propensity to form helical structure is somewhat higher for the AB region of the human protein, and it was suggested that differences in local helix propensity was an important factor in determining the relative stability. Although differing helical propensities may play a role in the different stability of the molten globules formed by human and bovine αLA, our analysis indicates that they cannot account for the drastic difference in the ability of our constructs to fold. In addition, the molten globule state formed by guinea pig αLA is more stable than that formed by the bovine protein, yet the AB region of bovine protein has a higher helical propensity while the helical propensity of the AB helical region of hen lysozyme is actually higher than that of bovine and guinea pig αLA yet hen lysozyme does not form a molten globule (*47*).

The structured regions of many molten globule states contain a large percentage of the hydrophobic core of the native state, suggesting that hydrophobic interactions are likely to be especially crucial for the formation of molten globule states (*48, 49*). These observations suggest that differences in hydrophobic character might contribute to the differing ability of the peptides to fold. Hydrophobicity is correlated with the burial of nonpolar surface area and ideally one would wish to calculate the change in solvent accessible surface area obtained for the folding of the constructs. Since the structures of the constructs are not known and are indeed likely to be fluctional, it is impossible to calculate the difference in buried surface area. Nonetheless, it is interesting to calculate the total accessible nonpolar surface area of each construct in an extended conformation since this gives some measure of the hydrophobic character of each molecule. The total accessible nonpolar surface area calculated for the two peptides that make up αLA:1−38/95−120 is 5% larger than the value for the lysozyme construct. The lysozyme construct is 6 residues longer than the αLA construct and the difference is larger (but still small) on a per residue basis. If the calculation is repeated using Gly−X−Gly peptides to model the unfolded structure, the difference between the two constructs is even smaller, less than 2% (*50*). These simple

calculations demonstrate that overall differences in the hydrophobicity of the side chains in two constructs is likely not the cause of the differing abilities to fold. Although the overall hydrophobicity of the side chains is likely to be important, it is clearly not the only factor that contributes to the inability of lys:1−40/98−127 to form a structured molten globule state. Further support for this conclusion is offered by an examination of the chimeric constructs. αLA:1−38/lys:98−127 is much more structured than lys:1−40/αLA:95−120, but the extended form of lys:1−40/αLA:95−120 contains more solvent accessible nonpolar surface area. The same conclusion is reached using the values from Gly−X−Gly peptides.

The distribution of polar and nonpolar groups within a protein is not uniform, and these comparisons provide only a gross overall picture of the properties of the respective peptide chains. Hence, it is of interest to compare the surface area buried by different regions in the context of the folded state, bearing in mind, of course, that the native structure is likely a poor representation of the conformation of the molten globule state. Nonetheless, it is interesting to determine if there are any clear differences that may correlate with the ability of the intact proteins to form a molten globule. In this context, it interesting to note that Freire and co-workers have concluded, based on detailed calorimetric measurements, that a larger percentage of the polar as compared to the nonpolar interactions present in the native state of αLA are disrupted in the molten globule state (*51*). Calculations of the amount of buried surface were performed using the extended chain to represent the unfolded state and the structure of the appropriate region of the crystal structure (all other atoms deleted) to represent the folded conformation. The A and B helices bury the most surface area of any two elements of secondary structure in the α-subdomain, consistent with the important role they play in determining the ability of the various constructs to fold. Intact lysozyme and αLA bury approximately the same amount of nonpolar surface area in the folded state, but lysozyme buries more polar surface area. The difference in the amount of buried polar surface area is largely localized to the core α-subdomain. The amount of nonpolar surface buried by this region is very similar for the two proteins (within 3%), but noticeably more polar surface area (2100 versus 1530 Å^2) is buried by this region of lysozyme. The difference in the burial of nonpolar surface area is not localized to one region of the core α-subdomain. The AB region of αLA and hen lysozyme considered in isolation bury approximately the same amount of nonpolar surface area, but the lysozyme AB region buries more polar surface area. The D/3$_{10}$ helical region of lysozyme also buries more polar surface area than does the same region of αLA. In contrast, the amount of polar and nonpolar surface area buried by the region composed of the β-subdomain, and the C helix of αLA (residues 39−100) is very similar to that buried by the same region of lysozyme (residues 41−104). The same conclusion is reached if only the region corresponding to the respective β-subdomains are considered. Thus, while there is no obvious correlation between the amount of nonpolar surface area buried and the ability to populate a molten globule state with a structured α-subdomain, there appears to be an inverse correlation between the burial of polar surface area and the ability to form a molten globule.

Very recently, Urvesky, Fink, and co-workers have analyzed the primary sequence of natively unfolded proteins and compared certain physical chemical properties of these sequences to the sequences of small proteins that are comparable of adopting a fixed tertiary structure (*52*). Remarkably, consideration of the normalized net charge and the mean hydrophobicity proved to be sufficient to distinguish between folded and natively unfolded sequences. Natively unfolded structures where found to populate a specific region of the plot of average charge vs mean hydrophobicity that corresponds to a region of overall low hydrophobicity and large charge. Interestingly, this analysis is also successful at predicting the properties of the constructs considered here. The lys:1−40 peptide has a noticeably higher normalized net charge and lower normalized Kyte−Doolittle hydrophobicity than does the αLA:1−38 fragment (*53*). All of the constructs that contain the lysozyme AB segment (lys:1−40) are predicted to be unfolded by their algorithm, while all of constructs that contain the αLA AB fragment (αLA:1−38) are predicted to be folded.

We have also analyzed the packing efficiencies of the α-domain of the native states of human αLA and hen lysozyme using the occluded surface algorithm of Fleming and co-workers (*32*). In this method, packing values vary from 0.0 for complete solvent exposure (no packing) to approximately 0.8 for maximally packed spheres (no units). It is important to note that these packing values are computed in the context of the native crystal structures. The average packing values of lysozyme and αLA are 0.36 and 0.35, respectively. These values are within the range typically observed in the structures of globular proteins solved by crystallographic methods (*33*, *54*). Clearly, the overall packing efficiencies do not correlate with the folding behavior, but again there are interesting localized differences. In particular, there is a difference in the average packing values of the two α-domains (excluding the C helix). The average residue packing value for the α-domain of αLA is 0.34. For hen lysozyme, the value is 0.39. This appears to be a significant difference since the packing values calculated for eight variants of lysozyme vary by at most 0.01 (*33*). There are also noticeably more residues in the lysozyme α-domain with very high packing values (>0.5) than in the α-domain of αLA. In the lysozyme α-domain, 17 residues have packing values above 0.5. In the αLA α-domain, only seven residues have packing values above 0.5. The residues that are the most highly packed in the core α-domain region of both lysozyme and αLA are at the A and B helix interface and within the B helix in the vicinity of the 28−111 disulfide bond. These calculations were performed using the structure of the native state of each protein, but similar results are obtained if the calculations are repeated using only residues 1−38 and 95−120 of αLA and residues 1−40 and 98−127 of lysozyme. The native state structure of these regions was used, and the rest of the protein was deleted. The average packing values are 0.34 for the lysozyme subdomain and 0.30 for the subdomain of αLA. The overall decrease is expected since part of the chain has been removed in these calculations. We repeated the calculation for just the AB helix region (all other portions of the proteins deleted), and again the lysozyme fragment appears to be better packed, 0.30 for lysozyme as compared to 0.25 for αLA. All of these calculations used the native state structures, and these almost

certainly do not represent the structural features of the molten globule state. Nevertheless, the difference in residue packing values is interesting and suggests one potential contributing factor for why intact αLA is more capable of forming a partially structured state with a stable, but loosely packed, partially folded structure in the α-subdomain. Privalov and co-workers have previously noted a correlation between the packing of equine and hen lysozyme and their unfolding behavior. The unfolding of equine lysozyme is less cooperative than hen lysozyme, and it forms a partially folded state at low pH. In equine lysozyme, there are two well-packed regions, one in the α- and one in the β-subdomain, which are separated by a loosely packed interface. In hen lysozyme, the interface is tightly packed, and there is a single extended cluster of well-packed residues (*55*). A recent study by Nussinov and colleagues has used a scoring function based upon compactness, degree of isolation, and hydrophobicity in an effort to dissection protein structures. They find, largely in agreement with the analysis presented here, that the α-lactalbumin fragment contain residues 1−38 linked to residues 106−123 scores very highly (*56*).

CONCLUSIONS

The results of the work presented here provide direct evidence that there is a clear difference in the ability of the isolated α-domains of lysozyme and αLA to form structure. Although the native structures are similar, the peptide construct from the α-domain of hen lysozyme is largely unstructured, while the human αLA peptide construct is highly helical and displays all the properties of a molten globule (*24*).

Our experiments with the four peptide constructs of lysozyme and αLA provides excellent suggestive evidence that much of the difference between the folding propensities of the lysozyme and αLA peptide constructs resides in the region containing the A and B helices. Of the four peptide constructs, only those that contain the AB helices of αLA (αLA:1−38/95−120 and αLA:1−38/lys:98−127) form significant structure. It is also noteworthy that the αLA:1−38 homodimer is the only homodimer that gains a large amount of additional helical structure upon oxidation. Our results are broadly consistent with recent site-specific mutagenesis studies but provide additional insight into the importance of the A and B helix region (*47, 57, 58*). Effective concentration measurements of the 28 to 111 disulfide have been used to gauge the effect of mutations in the α-subdomain of the molten globule state formed by a variant of α-lactalbumin that contains only the 28 to 111 disulfide. The majority of the residues that lead to a reduction in the effective concentration were located in the region of the A and B helices. That work together with the results presented here highlights the importance of this region and suggests that the A and B helices are a pivotal region that helps to differentiate the ability of human αLA to form a molten globule state from the inability of hen lysozyme to do so. The D and C-terminal 3_{10} helices do, nonetheless, play a role in stabilizing the molten globule of αLA. We have previously demonstrated that deletion of the D helix region or C-terminal 3_{10} helix region leads to a significant loss of structure (*24*). The data presented here suggest that the importance of these regions reflects relatively nonspecific interactions since both the αLA:1−38/lys:98−127 construct

and the αLA:1−38 homodimer are structured. The regions corresponding to the D helix and C-terminal 3_{10} helix may be necessary to protect exposed hydrophobic patches on the surface of the A and B helices and to form nonspecific interactions with residues in the A and B helices.

At first glance, our experiments that highlight a particularly critical role for the AB helix segment may appear to be in contrast to the earlier studies of Kim and Schulman (*59*). In fact, there is no inherent contradiction. In their experiments, a set of proline mutants were studied that involved proline substitutions in each of the helices of the α-subdomain of intact α-lactalbumin. Substitution with a proline decreased the overall helicity of the molten globule by the amount expected for the removal of the individual helix (except for the C-helix where proline substitutions had no noticeable effect). Disruption of each helix via proline substitution is not as drastic a probe as swapping entire regions of super secondary structure. In particular, the substitutions involved in the preparation of the chimeric constructs will alter the packing within the AB region and between the AB helix region and the D-3_{10} helical region. In addition, the α-subdomain construct studied here forms a less stable molten globule state than does the entire protein, and this should serve to amplify the effects of unfavorable substitutions. Taken together, the work reported here along with the earlier elegant studies of Kim and co-workers as well as our previous truncation studies helps to provide a unified view of the interactions that stabilize the molten globule state. The proline mutation experiments show that fully formed helices are not required; while our experiments using chimeric constructs together with our earlier studies of truncation constructs demonstrate that interactions involving these regions of the protein must be present to form the molten globule state (*24, 59*).

Our analysis of the primary sequences shows that local helix propensities or the hydrophobicity of the side chains while important cannot account for the different folding properties of the constructs. The arrangement of hydrophobic and hydrophilic residues in the primary sequence is certain to be important as are more subtle effects. In this regard, it is interesting that the α-subdomain of lysozyme buries more polar surface area in the native state and is better packed than the αLA α-subdomain.

ACKNOWLEDGMENT

REFERENCES

1. Kuwajima, K. (1989) *Proteins: Struct. Funct. Genet. 6*, 87−103.
2. Fink, A. L. (1995) *Annu. Rev. Biophys. Biomol. Struct. 24*, 495−522.
3. Ptitsyn, O. B. (1995) *Adv. Protein Chem. 47*, 83-217.
4. Privalov, P. L. (1996) *J. Mol. Biol. 258*, 707−725.
5. Arai, M., and Kuwajima, K. (2000) *Adv. Protein Chem. 53*, 209−271.

6. Creighton, T. E. (1997) *Trends Biochem. Sci. 22*, 6−10.

7. Kuwajima, K. (1996) *FASEB J. 10*, 102−108.

8. Chamberlain, A. K., and Marqusee, S. (2000) *Adv. Protein Chem. 53*, 283−328.

9. Uversky, V. N., and Ptitsyn, O. B. (1994) *Biochemistry 33*, 2782−2791.

10. Fink, A. L., Seshadri, S., and Oberg, K. A. (1997) *Folding Des. 3*, 19−25.

11. Uversky, V. N., and Ptitsyn, O. B. (1996) *J. Mol. Biol. 255*, 215−228.

12. Acharya, K. R., Ren, J., Stuart, D. I., Phillips, D. C., and Fenna, R. E. (1991) *J. Mol. Biol. 221*, 571−581.

13. Philips, D. C. (1974) in *Lysozyme* (Osserman, E. F., Canfield, R. E., and Beychock, S., Eds.) pp 9−30, Academic Press, New York.

14. Qasba, P. K., and Kumar, S. (1997) *CRC Crit. Rev. Biochem. 32*, 255−306.

15. Dobson, C. M., Evans, P. A., and Radford, S. E. (1994) *Trends Biochem. Sci. 19*, 31−37.

16. Ikeguchi, M., Kuwajima, K., Mitani, M., and Sugai, S. (1986) *Biochemistry, 25*, 6965−6972.

17. Kuwajima, K., Nitta, K., Yoneyama, M., and Sugai, S. (1976) *J. Mol. Biol. 106*, 359−373.

18. Tanford, C. (1970) *Adv. Prot. Chem. 24*, 1−95.

19. Baum, J., Dobson, C. M., Evans, P. A., and Hanley, C. (1989) *Biochemistry 28*, 7−13.

20. Chyan, C.-L., Wormald, C., Dobson, C. M., Evans, P. A., and Baum, J. (1993) *Biochemistry 32*, 5681−5691.

21. Schulman, B. A., Redfield, C., Peng, Z.-y., Dobson, C. M., and Kim, P. S. (1995) *J. Mol. Biol. 253*, 651−657.

22. Schulman, B. A., Kim, P. S., Dobson, C. M., and Redfield, C. (1997) *Nat. Struct. Biol. 4*, 630−634.

23. Peng, Z.-y., and Kim, P. S. (1994) *Biochemistry, 30*, 3248−3252.

24. Demarest, S. J., Boice, J. A., Fairman, R., and Raleigh, D. P. (1999) *J. Mol. Biol. 294*, 213−221.

25. de Laureto, P. P., Scaramella, E., Frigo, M., Wondrich, F. G., de Filippis, V., Zambonin, M., and Fontana, A. (1999) *Protein Sci. 8*, 1−14.

26. Pardon, E., Haezebrouck, P., De Baetselier, A., Hooke, S. D., Fancourt, K. T., Desmet, J., Dobson, C. M., Van Dael, H., and Joniau, M. (1995) *J. Biol. Chem. 270*, 10514−10524.

27. Mizuguchi, M., Masaki, K., and Nitta, K. (1999) *J. Mol. Biol. 292*, 1137−1148.

28. Masaki, K., Masuda, R., Takase, K., Kawano, K., and Nitta, K. (2000) *Protein Eng. 13*, 1−4.

29. Mizuguchi, M., Masaki, K., Demura, M., and Nitta, K. (2000) *J. Mol. Biol. 298*, 985−995.

30. Pace, C. N., Vajdos, F., Fee, L., Grimsley, G., and Gray, T. (1995) *Protein Sci. 4*, 2411−2423.

31. Cohn, E. J., and Edsall, J. T. (1943) *Proteins, Amino Acids and Peptides as Ions and Dipolar Ions*, Reinhold Publishing Coorporation, New York.

32. Pattabiraman, N., Ward, K. B., and Fleming, P. J. (1995) *J. Mol. Recognit. 8*, 334−344.

33. Fleming, P. J., and Richards, F. M. (2000) *J. Mol. Biol. 299*, 487−498.

34. Munoz, V., and Serrano, L. (1997) *Biopolymers 41*, 495−509.

35. Lacroix, E., Viguera, A. R., and Serrano, L. (1998) *J. Mol. Biol. 284*, 173−191.

36. Yang, J. J., Buck, M., Pitkeathly, M., Kotik, M., Haynie, D. T., Dobson, C. M., and Radford, S. E. (1995) *J. Mol. Biol. 252*, 483−491.

37. Yang, J. J., van den Berg, B., Pitkeathly, M., Smith, L. J., Bolin, K. A., Keiderking, T. A., Redfield, C., Dobson, C. M., and Radford, S. E. (1996) *Folding Des. 1*, 473−484.

38. Semisotnov, G. V., Rodionova, N. A., Razgulyaev, O. I., Uversky, V. N., Gripas, A. F., and Gilmanshin, R. I. (1991) *Biopolymers 31*, 119−128.

39. Ali, V., Prakash, K., Kulkarni, S., Ahmad, A., Madhusudan, K. P., and Bhakuni, V. (1999) *Biochemistry 38*, 13635−13642.

40. Gast, K., Zirwer, D., Welfle, H., Bychkova, V. E., and Ptitsyn, O. B. (1986) *Int. J. Biol. Macromol. 8*, 231−236.

41. Wilkins, D. K., Grimshaw, S. B., Receveur, V., Dobson, C. M., Jones, J. A., and Smith, L. J. (1999) *Biochemistry 38*, 16424−16431.

42. Uversky, V. N. (1993) *Biochemistry 32*, 13288−13295.

43. Demarest, S. J., Fairman, R., and Raleigh, D. P. (1998) *J. Mol. Biol. 283*, 279−291.

44. Demarest, S. J., Hua, Y., and Raleigh, D. P. (1999) *Biochemistry 38*, 7380−7387.

45. Demarest, S. J., and Raleigh, D. P. (2000) *Proteins: Struct. Funct. Genet. 38*, 189−196.

46. Moriarty, D. F., Demarest, S. J., Robblee, J., Fairman, R. F., and Raleigh, D. P. (2000) *Biochim. Biophys. Acta 1476*, 9−19.

47. Uchiyama, H., Perez-Prat, E. M., Watanabe, K., Kumagai, I., and Kuwajima, K. (1995) *Protein Eng. 8*, 1153−1161.

48. Dill, K. A. (1990) *Biochemistry 29*, 7133−7155.

49. Haynie, D. T., and Freire, E. (1993) *Proteins: Struct. Funct. Genet. 16*, 115−140.

50. Livingstone, J. R., Spolar, R. S., and Record, M. T. (1991) *Biochemistry 30*, 4237−4244.

51. Freire, F. (1995) *Annu. Rev. Biophys. Biomol. Struct. 24*, 141−165.

52. Uversky, V. N., Gillespie, J. R., and FInk, A. L. (2000) *Proteins: Struct. Funct. Genet. 41,* 415−427.

53. Kyte, J., and Doolittle, R. F. (1982) *J. Mol. Biol. 157*, 105−132.

54. Ratnaparkhi, G. S., Ramachandran, S., Udgaonkar, J. B., and Varadarajan, R. (1998) *Biochemistry 37*, 6958−6966.

55. Griko, Y. V., Freire, E., Privalov, G., Van Deal, H., and Privalov, P. L. (1995) *J. Mol. Biol. 252,* 447−459.

56. Tsai, C.-J., Maizel, J. V., and Nussinov, R. (2000) *Proc. Acad. Sci. U.S.A. 97*, 12038−12043.

57. Song, J., Bai, P., Luo, L., and Peng, Z.-y. (1998) *J. Mol. Biol. 280*, 167−174.

58. Wu, L. C., and Kim, P. S. (1998) *J. Mol. Biol. 280*, 175−182.

59. Schulman, B. A, and Kim, P. S. (1996) *Nat. Struct. Biol. 3*, 682−687

60. Kraulis, P. J. (1991) *J. Appl. Crystallogr. 24*, 946−950.

61. Acharya, K. R., Stuart, D. I., Walker, N. P. C., Lewis, M., and Phillips, D. C. (1989) *J. Mol. Biol. 208*, 99−127.